

# The Effects of Age and Cx<sub>3</sub>cr1 Deficiency on Retinal Microglia in the *Ins2<sup>Akita</sup>* Diabetic Mouse

Jelena Marie Kezic,<sup>1,2</sup> Xiangting Chen,<sup>1</sup> Elizabeth P. Rakoczy,<sup>3,4</sup> and Paul G. McMenamin<sup>1</sup>

**PURPOSE.** Diabetic retinopathy (DR) is a major cause of visual impairment in developed countries. While DR has been described classically as a microvascular disease, recent evidence suggests that changes to retinal microglia are an early feature of retinopathy. In our study, we assessed changes in microglial distribution and morphology in vivo and ex vivo in a mouse model of non-proliferative DR, and further examined effects of age and the absence of the functional chemokine receptor Cx<sub>3</sub>cr1 on the progression of these changes.

**METHODS.** To isolate the effects of the three variables: diabetic status, age, and role of Cx<sub>3</sub>cr1, the *Ins2<sup>Akita</sup>* mouse was crossed with Cx<sub>3</sub>cr1-eGFP reporter mice. Eyes were assessed clinically in vivo at 10, 20, 30, and 46 weeks of age, and the retinal structure and arrangement of GFP<sup>+</sup> microglia was examined ex vivo using whole mount immunofluorescence staining and confocal microscopy.

**RESULTS.** Clinical examination of the fundus, vasculature, or GFP<sup>+</sup> microglial distribution did not reveal any macroscopic changes related to diabetic status; however, ex vivo microscopic analysis revealed alterations in microglial network organization, and evidence of cell shape changes regarded classically as signs of activation, in *Ins2<sup>Akita</sup>* mice from 10 weeks of age. These changes were exacerbated in older diabetic mice whose microglia lacked Cx<sub>3</sub>cr1 (*Ins2<sup>Akita</sup> Cx<sub>3</sub>cr1<sup>slp/slp</sup>* mice). Diabetic status and Cx<sub>3</sub>cr1 deficiency led to accumulations of Iba-1<sup>+</sup> hyalocytes (vitreal macrophages) and subretinal macrophages.

**CONCLUSIONS.** These data showed that changes to murine retinal microglia occur in response to systemic diabetic status in the

absence of overt retinopathy and inflammation. These changes are exaggerated in mice lacking Cx<sub>3</sub>cr1, suggesting fractalkine-Cx<sub>3</sub>cr1 interactions may have a role in early neuronal changes in preproliferative DR. (*Invest Ophthalmol Vis Sci.* 2013; 54:854–863) DOI:10.1167/iovs.12-10876

Diabetic retinopathy (DR), a secondary complication of type 1 diabetes mellitus and type 2 diabetes, is the leading cause of blindness in working age adults.<sup>1</sup> Studies in the United States and Australia have estimated that between 50 and 97% of patients with type 1 diabetes suffer retinopathy by 15 to 20 years post diagnosis,<sup>2</sup> while an estimated 40% of patients with type 2 diabetes show signs of DR.<sup>3</sup> With the prevalence of type 2 diabetes set to rise due to the increasing problem of obesity in developed and developing nations, the number of patients with diabetes at risk of development of DR also is likely to increase. As such, novel therapeutic targets are essential to reduce the global impact of this vision-threatening disease. Presently, few options are available for the early background or non-proliferative phase of DR, and current treatments for DR, such as laser therapy, are targeted towards the active vasoproliferative phase.<sup>4</sup> Although DR traditionally has been described as a microvascular disease, recent evidence from rodent studies suggests a strong inflammatory component, with early features of inflammation having been identified, including leukostasis, glycation end-product formation, increased production of nitric oxide, and proinflammatory cytokines, together with morphologic changes in retinal microglia.<sup>5–9</sup>

Microglia are a specialized population of macrophages resident in central nervous system (CNS) tissue, including the retina. Resting microglia perform homeostatic functions associated with host defense and tissue repair,<sup>10,11</sup> whereas “primed” microglia can exert neuroprotective effects through the release of trophic and anti-inflammatory factors, including interleukin (IL)-10 and transforming growth factor-beta 1 (TGF-β1).<sup>12</sup> Upon activation in response to conditions of metabolic stress, injury, or inflammation, microglia upregulate immune markers, including MHC Class II, CD68, and isolectin-B4 (IB4), generate reactive oxygen species, and produce a number of inflammatory cytokines, including tumor necrosis factor-alpha (TNF-α), IL-6, IL-1β, and IL-12p40.<sup>12,13</sup> These functional changes in microglia have been reported to exert neurotoxic effects in numerous disease models with a neuroimmunologic pathogenesis, including Alzheimer’s disease, multiple sclerosis, and Parkinson’s disease.<sup>14–17</sup> In the context of the eye, a similar mechanism has been proposed for microglia as potential mediators of vascular damage in DR.<sup>18,19</sup> As well as these functional changes, the morphologic transformation of microglia in response to inflammation or injury has been well documented, with resting or highly ramified microglia assuming a reactive or less branched appearance upon activation.<sup>20,21</sup> Morphologic changes in microglia have been reported before the occurrence of neuronal cell death or

From the <sup>1</sup>Department of Anatomy and Developmental Biology, Monash University, Clayton, Victoria, Australia; the <sup>2</sup>Centre for Eye Research Australia, Department of Ophthalmology, University of Melbourne, Royal Victorian Eye and Ear Hospital, East Melbourne, Victoria, Australia; the <sup>3</sup>Centre for Ophthalmology and Visual Science, University of Western Australia, Crawley, Australia; and the <sup>4</sup>Department of Molecular Ophthalmology, Lions Eye Institute, Nedlands, Australia.

Supported by an NHMRC project Grant #634469, by The Rebecca L. Cooper Foundation Ltd. for some of the equipment purchased for use in this study, and by Operational Infrastructure Support from the Victorian Government (Centre for Eye Research Australia). Supported partially by the National Health and Medical Research Council Centre for Clinic Research Excellence #529923 – Translational Clinic Research in Major Eye Diseases (JMK).

Submitted for publication August 30, 2012; revised November 19, December 18, and December 29, 2012; accepted December 31, 2012.

Disclosure: J.M. Kezic, None; X. Chen, None; E.P. Rakoczy, None; P.G. McMenamin, None

Corresponding author: Paul G. McMenamin, Department of Anatomy and Developmental Biology, School of Biomedical Sciences, Monash University, Wellington Road, Clayton, VIC 3800, Australia; paul.mcmnamin@monash.edu.

vascular changes in DR in tissues samples from human retinæ and rodent models of the disease.<sup>7,18</sup> Thus, we proposed that morphologic changes to microglia in the diabetic retina may be a potential early response to hyperglycemia.

Cx<sub>3</sub>cr1, the receptor for the chemokine fractalkine (Cx<sub>3</sub>cl1), is expressed at high levels on tissue resident monocyte-derived cells, including retinal microglia, and is involved in the migration of myeloid cells along either gradients of soluble fractalkine released by or expressed on injured neurones, thereby having a protective role in the normal nervous system.<sup>22,23</sup> Cx<sub>3</sub>cr1<sup>+/-gfp</sup> and Cx<sub>3</sub>cr1<sup>gfp/gfp</sup> reporter mice have been used extensively to investigate the role of this chemokine receptor in a variety of neurologic and non-neurologic conditions.<sup>22-26</sup> Using this experimental model, the absence of Cx<sub>3</sub>cr1 on microglia has been shown to accelerate neuronal cell death in mouse models of neuroinflammation, including Parkinson's disease, amyotrophic lateral sclerosis, and lipopolysaccharide (LPS)-induced inflammation.<sup>23</sup>

The primary purpose of our study was to determine whether microglia are altered in DR with age, and whether these changes are influenced by the absence of Cx<sub>3</sub>cr1. In light of the known effects of Cx<sub>3</sub>cr1 deficiency in accelerating neuronal degenerative conditions, we hypothesized that Cx<sub>3</sub>cr1 deficiency on resident microglia may accelerate the development of retinal vascular and neuronal changes in the *Ins2<sup>Akita</sup>* mouse. Previously, studies using *Ins2<sup>Akita</sup>* mice have reported retinal changes, including increased vascular permeability and microglial reactivity within 3 months of age.<sup>9</sup> To investigate these issues, we produced a novel mouse model by crossing *Ins2<sup>Akita</sup>* mice<sup>9,27</sup> with Cx<sub>3</sub>cr1<sup>gfp/gfp</sup> mice<sup>22</sup> to produce "Green Akita" mice. These mice either maintained a functional Cx<sub>3</sub>cr1 (*Ins2<sup>Akita</sup>* Cx<sub>3</sub>cr1<sup>+/-gfp</sup>) or were deficient in the receptor (*Ins2<sup>Akita</sup>* mice with Cx<sub>3</sub>cr1<sup>gfp/gfp</sup>). This unique model allows for the long-term in vivo assessment of microglia and obviates the need for immunofluorescence staining of retinal microglia ex vivo.

Our report illustrates morphologic changes to a subpopulation of microglia, in addition to a marked disruption to the regular three-dimensional laminar microglial networks in *Ins2<sup>Akita</sup>* mice from 10 weeks of age. Deficiency in Cx<sub>3</sub>cr1, while not leading to overt vascular changes or retinal thinning, does accelerate these microglial responses in the diabetic retina. The accumulation of Iba-1<sup>+</sup> hyalocytes (macrophages at the retinal-vitreous interface) and subretinal macrophages in the diabetic retina, likely derived from activated microglia, appears to indicate that retinal macrophage activation is a prodromal feature of retinopathy.

## MATERIALS AND METHODS

### Experimental Animals

Cx<sub>3</sub>cr1-eGFP mice, in which monocyte-derived cells are GFP<sup>+</sup>, were crossed with *Ins2<sup>Akita</sup>* mice. Male nondiabetic Cx<sub>3</sub>cr1<sup>+/-gfp</sup> and Cx<sub>3</sub>cr1<sup>gfp/gfp</sup> littermates acted as controls. C57BL/6J Cx<sub>3</sub>cr1<sup>+/-gfp</sup> and Cx<sub>3</sub>cr1<sup>gfp/gfp</sup> (Cx<sub>3</sub>cr1-deficient) transgenic mice, originally obtained from Dr Steffen Jung (Weizmann Institute of Science, Rehovot, Israel),<sup>22</sup> were bred at the Animal Research Laboratory (Monash University, Clayton, VIC, Australia) and maintained on 12-hour day/night cycles, with free access to food and water. All procedures conformed to the Association for Research in Vision and Ophthalmology (ARVO) Statement for the Use of Animals in Ophthalmic and Vision Research, and were approved by the Monash University Animal Ethics Committee. Only males carrying a single *Ins2<sup>Akita</sup>* allele are established as suitable models of diabetic complications as their female counterparts experience an inconsistent diabetic phenotype. *Ins2<sup>Akita</sup>*

homozygotes die in early life, preventing their use as models of chronic hyperglycemia. Our *Ins2<sup>Akita</sup>* colony was derived from commercially available breeders (Jackson Laboratories, Bar Harbor, ME). The Cx<sub>3</sub>cr1 and *Ins2<sup>Akita</sup>* mice used in our study were on a C57BL/6J background (wt/wt when screened for the *rd8* mutation in the *Crb1* gene).<sup>28</sup> Four groups of mice (nondiabetic Cx<sub>3</sub>cr1<sup>gfp/+</sup> and Cx<sub>3</sub>cr1<sup>gfp/gfp</sup>, and diabetic Cx<sub>3</sub>cr1<sup>gfp/+</sup> *Ins2<sup>Akita</sup>* and Cx<sub>3</sub>cr1<sup>gfp/gfp</sup> *Ins2<sup>Akita</sup>*) were produced by breeding and genotyping to verify *Ins2* gene mutation, and Cx<sub>3</sub>cr1 deficiency was performed following established protocols.<sup>28,29</sup> Diabetic animals were not treated with insulin.

### Glycosylated Hemoglobin

To confirm diabetic status of *Ins2<sup>Akita</sup>* mice, glycated hemoglobin (HbA1c) was measured as described previously<sup>27</sup> using a Siemens DCA 2000<sup>+</sup> Analyzer (Siemens Medical Solutions Diagnostics, Bayswater, VIC, Australia).

### In Vivo Retinal Fundus Imaging

Clinical imaging was performed on anesthetized mice (ketamine/xylazine) using a Micron III camera (Phoenix Research Laboratories, San Ramon, CA). To dilate the pupils, eyes were moistened using drops containing 0.5% tropicamide (Alcon Australia, Frenchs Forest, Australia). A lubricating gel (Viscotears; Novartis Pharmaceuticals, Australia Pty Limited, North Ryde, NSW, Australia) was placed on the microscope objective to prevent drying of the cornea. Then, 20-second videos were captured for both eyes in bright field and fluorescence modes before fluorescein angiography was performed, for which 20 µL of 10% sodium fluorescein (Alcon Australia) were injected subcutaneously. Mice were imaged at 10, 20, 30, and 46 weeks of age, and groups (*n* = 4-6 animals) were sacrificed immediately after retinal imaging for ex vivo analysis.

### Tissue Collection and Fixation

Mice were euthanized by intraperitoneal injection with sodium pentobarbitone (100 mg/kg; Virbac, Carindale, QLD, Australia) and fixed by intracardial perfusion with 4% paraformaldehyde (PFA) as described previously.<sup>30</sup> One eye was postfixed in 4% PFA for immunofluorescence staining of retinal whole mounts, while the fellow eye was postfixed in Karnovsky's fixative (4% PFA, 1% glutaraldehyde) for resin embedding and histologic analysis.

### Histologic Analysis

Eyes were embedded in glycol methacrylate (GMA) medium and sectioned (5 µm) in the sagittal plane at three different levels close to the optic nerve-pupillary axis. Sections were stained using hematoxylin and eosin (H&E), and imaged using Aperio ScanScope digital slide scanner (400× magnification; Aperio, Vista, CA). The marginal and central retinal thicknesses were measured 300 µm from the ciliary body and optic nerve, respectively, using Aperio Imagescope viewer software. Average thickness measurements for each eye were obtained from three different sections and data pooled per group (*n* = 4 animals per group).

### Immunofluorescence Staining and Confocal Microscopy

Retinal whole mounts were prepared as documented previously.<sup>31</sup> Briefly, tissues were incubated in 20 mM EDTA tetrasodium (37°C) for 30 minutes, then blocked for 60 minutes at room temperature (RT) with 3% BSA and 0.3% Triton-X solution in PBS. Tissues were treated with one of the following antibodies: polyclonal rabbit anti-Iba-1 (ionized calcium binding adaptor molecule 1; Wako Pure Chemical Industries, Ltd., Osaka, Japan), biotinylated isolectin-B4 (Vector Laboratories, Burlingame, CA), mouse anti-GFAP (BD Pharmingen, San Diego, CA) and rat

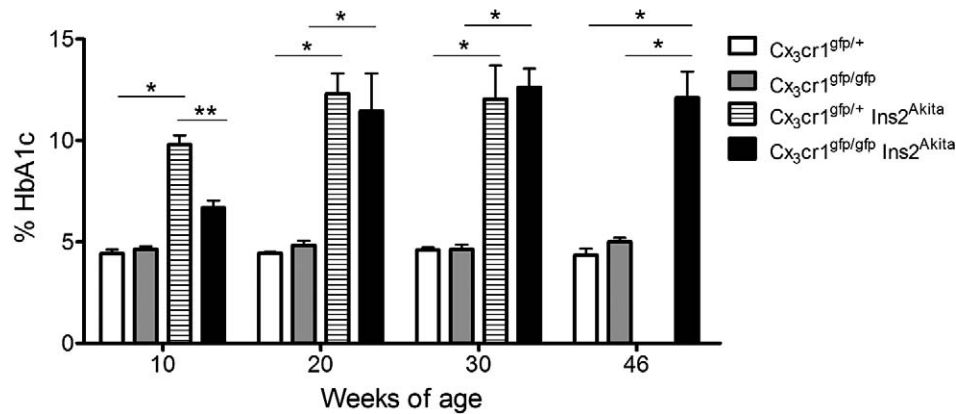


**FIGURE 1.** HbA1c measurements. Mean levels of HbA1c in nondiabetic (*Cx<sub>3</sub>cr1<sup>gfp/+</sup>* and *Cx<sub>3</sub>cr1<sup>gfp/gfp</sup>*) mice and diabetic (*Cx<sub>3</sub>cr1<sup>gfp/+</sup> Ins2<sup>Akita</sup>* and *Cx<sub>3</sub>cr1<sup>gfp/gfp</sup> Ins2<sup>Akita</sup>*) mice.  $n = 4$  to 6 per group per time point. Error bars indicate SEM. \* $P < 0.05$ , \*\* $P < 0.005$ .

anti-mouse MHC Class II (M5/114; BD Pharmingen) at 4°C overnight. Samples then were incubated with biotin-conjugated anti-rat (1:300; Amersham Biosciences, Piscataway, NJ), biotin-conjugated anti-rabbit (1:300; Vector Laboratories) antibody, or anti-mouse Alexa Fluor 568 (1:400; Molecular Probes, Eugene, OR) for 2 hours at RT. Samples treated with biotinylated antibodies were incubated for 2 hours (RT) with streptavidin-conjugated Cy3 (Jackson ImmunoResearch, West Grove, PA). Hoescht was used for nuclear staining. Retinae were mounted on slides with the vitreous side up. Immunostained whole mounts were imaged using epifluorescence (Olympus Provis Ax70 microscope, SIS AnalySis software; Olympus, Mount Waverley, VIC, Australia) and confocal microscopy (Nikon C1 Upright; Nikon, Sydney, NSW, Australia). Confocal microscopic images spanning the full thickness of retinal tissue were prepared by scanning at 1 μm increments (20× objective lens). To calculate density of hyalocytes and subretinal macrophages, six epifluorescence images from randomly selected areas of anti-Iba-1 stained whole mount tissues were taken at the level of the nerve fiber (NFL) and photoreceptor cell (PCL) layers, respectively, and counted by a masked observer. Microglial cell number was calculated using ImageJ software (available in the public domain at <http://rsbweb.nih.gov/ij/>). Imaris software (Imaris Suite, version 7.4; Bitplane, Inc., South Windsor, CT) was used to calculate microglial dendrite distance/extension from the soma. All measurements were done in a masked fashion. Final image processing was performed using Adobe Photoshop (Version 7.0; Adobe Systems, Inc., San Jose, CA).

### Statistical Analysis

All data were analyzed by two-way ANOVA followed by Tukey's multiple comparison test (5% significance level, GraphPad Prism Version 4.01 Software; GraphPad, San Diego, CA). For HbA1c, microglial cell number and dendrite distance from soma measurements, individual parameters within age groups were analyzed using unpaired Student's *t*-test ( $P < 0.05$  considered as significant). Data are presented as mean ± SEM.

## RESULTS

### Cx<sub>3</sub>cr1 Deficiency Influences the Development of Hyperglycemia in *Ins2<sup>Akita</sup>* Mice

To confirm diabetic status in *Ins2<sup>Akita</sup>* mice, HbA1c was measured across groups. Although elevated HbA1c levels (≥6%) were detected from 10 to 46 weeks of age in all diabetic mice (Fig. 1), HbA1c levels in *Cx<sub>3</sub>cr1<sup>gfp/gfp</sup> Ins2<sup>Akita</sup>* mice were notably lower than those measured in *Cx<sub>3</sub>cr1<sup>+/gfp</sup> Ins2<sup>Akita</sup>* mice at 10 weeks ( $P < 0.005$ ). These data suggested that Cx<sub>3</sub>cr1 deficiency delays full development of hyperglyce-

mia in *Ins2<sup>Akita</sup>* mice. No differences were observed in HbA1c measurements between *Cx<sub>3</sub>cr1<sup>gfp/+</sup> Ins2<sup>Akita</sup>* and *Cx<sub>3</sub>cr1<sup>gfp/gfp</sup> Ins2<sup>Akita</sup>* mice at 20 and 30 weeks of age.

### No Overt Changes to the Retinal Fundus or Vasculature Were Detected by In Vivo Imaging of *Ins2<sup>Akita</sup>* Mice

In vivo retinal imaging was performed in nondiabetic (*Cx<sub>3</sub>cr1<sup>gfp/+</sup>* and *Cx<sub>3</sub>cr1<sup>gfp/gfp</sup>*) and diabetic (*Cx<sub>3</sub>cr1<sup>gfp/+</sup> Ins2<sup>Akita</sup>* and *Cx<sub>3</sub>cr1<sup>gfp/gfp</sup> Ins2<sup>Akita</sup>*) mice. Bright field assessment revealed no overt changes to the mouse fundus at 10 (Fig. 2A), 20, and 30 (see Supplementary Material and Supplementary Fig. S1, <http://www.iovs.org/lookup/suppl/doi:10.1167/iovs.12-10876/-/DCSupplemental>) weeks of age. At 46 weeks, focal whitish lesions were observed in *Cx<sub>3</sub>cr1<sup>gfp/gfp</sup>* and *Cx<sub>3</sub>cr1<sup>gfp/gfp</sup> Ins2<sup>Akita</sup>* mice (Fig. 2B), but not *Cx<sub>3</sub>cr1<sup>gfp/+</sup>* mice (not shown), indicating these changes were associated with Cx<sub>3</sub>cr1-deficiency as described previously.<sup>32,33</sup> These focal lesions were more pronounced in *Cx<sub>3</sub>cr1*-deficient *Ins2<sup>Akita</sup>* mice (Fig. 2B), suggesting diabetes may accelerate these retinal changes, and likely are representative of subretinal macrophage accumulation, which is a well documented phenomenon in Cx<sub>3</sub>cr1-deficient mice with aging.<sup>32,34,35</sup> In vivo fluorescence imaging of the retina at 10 (Fig. 3A), 20, and 30 (see Supplementary Material and Supplementary Fig. S1, <http://www.iovs.org/lookup/suppl/doi:10.1167/iovs.12-10876/-/DCSupplemental>) weeks revealed no overt alterations to the geographic distribution of microglia with age and, furthermore, no vascular leakage was detected by fluorescein angiography in either nondiabetic or diabetic mice at all time points examined (Fig. 3B; see Supplementary Material and Supplementary Fig. S1, <http://www.iovs.org/lookup/suppl/doi:10.1167/iovs.12-10876/-/DCSupplemental>).

### Disruption of the Regular Arrangement of Microglia Occurs in the Diabetic Retina Independent of Cx<sub>3</sub>cr1 Signaling

While we did not detect changes in the overall distribution of retinal microglia by in vivo imaging (Fig. 3), previous microscopic studies on frozen sections have noted morphologic alterations to microglia in *Ins2<sup>Akita</sup>* mice.<sup>9</sup> To characterize these microglial changes more closely, confocal microscopic analysis was performed on retinal whole mounts (Figs. 4, 5). In the retina of nondiabetic mice microglia are distributed regularly in the NFL/ganglion cell layer (GCL), inner plexiform layer (IPL), and outer plexiform layer (OPL; Fig. 4A, left). Assessment of confocal

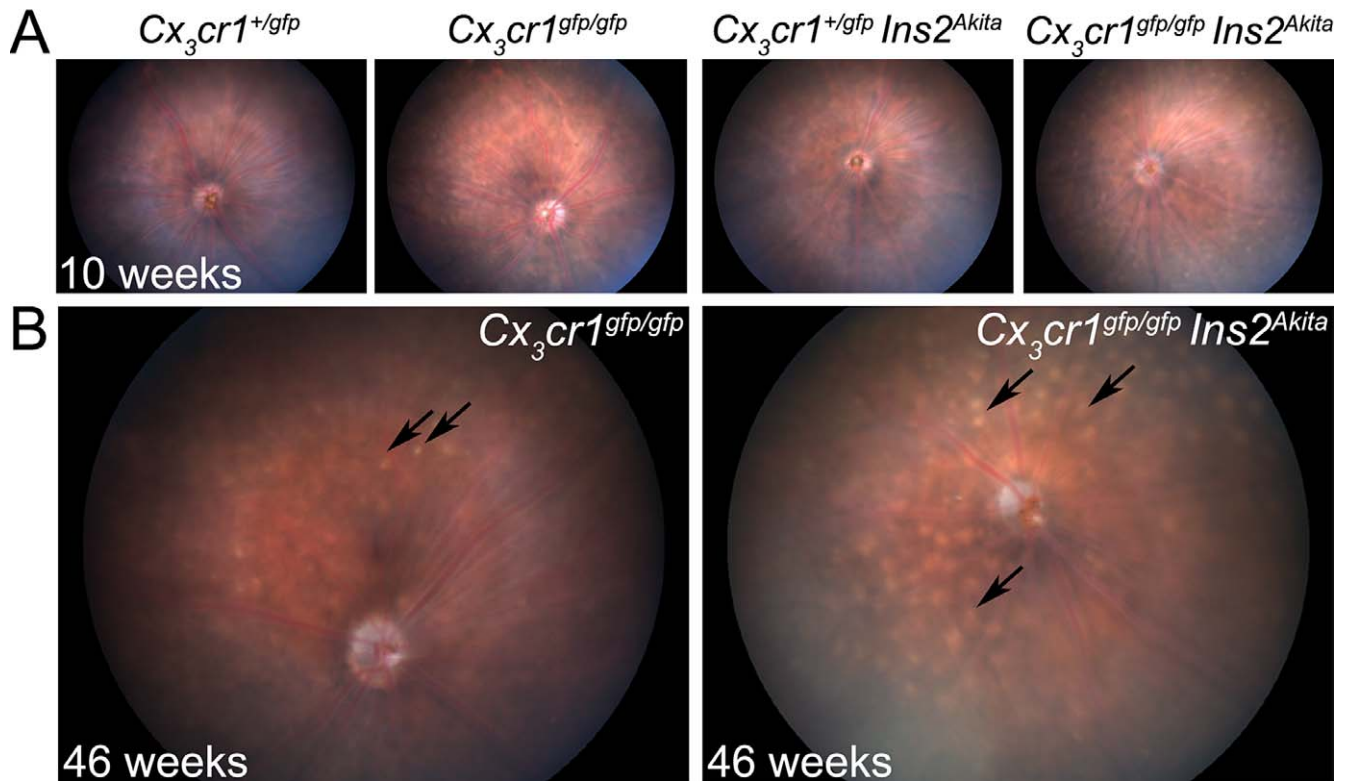


**FIGURE 2.** In vivo retinal imaging. Clinical assessment of nondiabetic (*Cx<sub>3</sub>cr1<sup>+/gfp</sup>* and *Cx<sub>3</sub>cr1<sup>gfp/gfp</sup>*) and diabetic (*Cx<sub>3</sub>cr1<sup>+/gfp</sup> Ins2<sup>Akita</sup>* and *Cx<sub>3</sub>cr1<sup>gfp/gfp</sup> Ins2<sup>Akita</sup>*) mice using the Micron III retinal imaging system. Images are representative snapshots extracted from 20-second videos. Bright field assessment of the mouse fundus at 10 weeks of age (A) revealed no overt changes associated with *Cx<sub>3</sub>cr1* deficiency or hyperglycemia. Focal deposits (black arrows) were observed in *Cx<sub>3</sub>cr1<sup>gfp/gfp</sup>* and *Cx<sub>3</sub>cr1<sup>gfp/gfp</sup> Ins2<sup>Akita</sup>* mice at 46 weeks, being more pronounced in diabetic mice (B).

scans spanning the full thickness of the retina and viewed in side profile revealed a marked disruption of the normal laminar arrangement of microglia in *Ins2<sup>Akita</sup>* mice from 10 weeks of age (Fig. 4A, right). This disruption in microglial architecture and distribution became more evident with age (Figs. 4B–D). In nondiabetic mice, a distinct band lacking GFP<sup>+</sup> microglia,

representative of the outer nuclear layer (ONL), was apparent between the IPL and OPL, with few microglial processes or cell bodies extending into this layer. The distinct separation of IPL and OPL microglial populations was lost in diabetic mice (Figs. 4A–D). The cellular processes extending through the nuclear layers were visualized more readily in 3 dimensions using Imaris

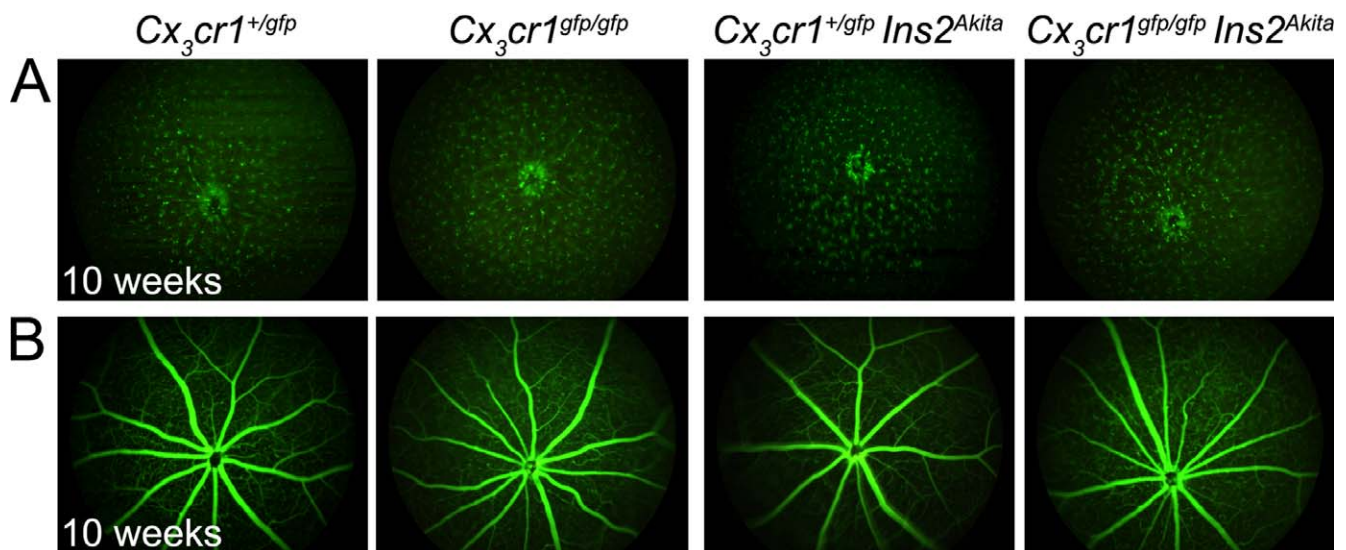


**FIGURE 3.** In vivo retinal imaging of microglia and fluorescein angiography. Clinic assessment using the Micron III retinal imaging system. Images are representative snapshots extracted from 20-second videos at the 10-week time point. Fluorescence examination of the mouse fundus at 10 weeks of age revealed no changes to the normal distribution of retinal microglia (A). No vascular leakage was detected by fluorescein angiography (B). Images are representative of 4 to 6 mice per group for each time point.

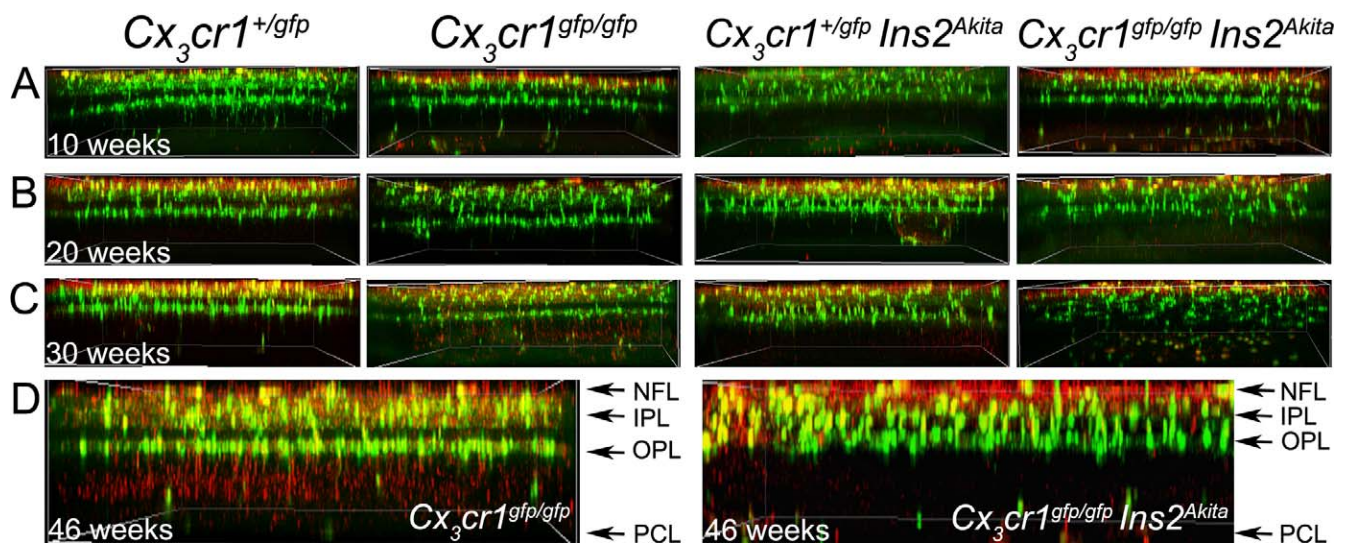


**FIGURE 4.** Disruption of microglial architecture in the retina of *Ins2<sup>Akita</sup>* mice. Confocal microscopic images representative of whole retinal scans from NFL to PCL viewed in side profile. Scans were collected at 1  $\mu$ m increments. Whole retinæ were imaged from nondiabetic (*Cx<sub>3</sub>cr1<sup>+/gfp</sup>* and *Cx<sub>3</sub>cr1<sup>gfp/gfp</sup>*) and diabetic (*Cx<sub>3</sub>cr1<sup>+/gfp</sup> Ins2<sup>Akita</sup>* and *Cx<sub>3</sub>cr1<sup>gfp/gfp</sup> Ins2<sup>Akita</sup>*) mice at 10 (A), 20 (B), 30 (C), and 46 (D) weeks of age. Note the disruption of microglial architecture in the IPL and OPL of diabetic mice as early as 10 weeks of age, in that the distinct space between the IPL and OPL representative of the inner nuclear layer and normally devoid of microglia is less apparent. *Green*: GFP<sup>+</sup> microglia *Red*: Iba-1 immunofluorescence staining.

software (see Supplementary Material and Supplementary Videos 1, 2, <http://www.iovs.org/lookup/suppl/doi:10.1167/iovs.12-10876/-/DCSupplemental>). To examine whether changes in microglial cell number accompanied the disruption of normal microglial architecture, the density of microglia in the NFL, IPL, and OPL was compared in nondiabetic and diabetic mice. No significant differences were observed at any of the time points examined (see Supplementary Material and Supplementary Fig. S2, <http://www.iovs.org/lookup/suppl/doi:10.1167/iovs.12-10876/-/DCSupplemental>).

### Retinal Microglia Changes in Diabetic Mice are Enhanced if They Lack the Chemokine Receptor *Cx<sub>3</sub>cr1*

We originally postulated that pre-proliferative changes in the diabetic retina of the *Ins2<sup>Akita</sup>* mouse would be augmented in mice lacking the chemokine receptor *Cx<sub>3</sub>cr1*. Therefore, we next analyzed the morphologic changes to microglial cell populations within the individual retinal layers in *Cx<sub>3</sub>cr1<sup>+/gfp</sup> Ins2<sup>Akita</sup>* and *Cx<sub>3</sub>cr1<sup>gfp/gfp</sup> Ins2<sup>Akita</sup>* mice. In the former group, whose microglia express the chemokine receptor, the microglia displayed a normal ramified morphology and laminar distribution at 10 weeks of age (not shown). In *Cx<sub>3</sub>cr1<sup>gfp/gfp</sup> Ins2<sup>Akita</sup>* mice, microglia in the IPL (not shown) and OPL exhibited two distinct morphologies: ramified and reactive (Fig. 5A). Ramified microglia in diabetic mice were of similar morphology to those present in nondiabetic mice; however, reactive microglia had fewer branching dendrites and primary dendrites appeared shorter or retracted when compared to ramified microglia (Fig. 5, arrowheads). A subpopulation of reactive microglia were present in *Cx<sub>3</sub>cr1<sup>+/gfp</sup> Ins2<sup>Akita</sup>* and *Cx<sub>3</sub>cr1<sup>gfp/gfp</sup> Ins2<sup>Akita</sup>* mice at 20 (Fig. 5B) and 30 (Fig. 5C) weeks of age, and in *Cx<sub>3</sub>cr1<sup>+/gfp</sup> Ins2<sup>Akita</sup>* retinæ at 46 weeks (Fig. 5C).

Changes in microglial morphology, especially alterations to the volume of perinuclear cytoplasm and thickened, shortened, less ramified processes, have been correlated with an activated functional state.<sup>12,36,37</sup> Therefore, in our study, we characterized further the morphologic changes to microglia in the diabetic mouse retina by quantifying the distance of

primary dendrites from the cell body of OPL reactive and ramified microglia (Fig. 5D). The length of dendrites of reactive microglia in diabetic mice was significantly less than when compared to those of ramified microglia at all time points examined (Fig. 5D). Interestingly, at 30 weeks, dendrite length of ramified microglia in *Cx<sub>3</sub>cr1<sup>+/gfp</sup> Ins2<sup>Akita</sup>* mice was significantly lower when compared to the length of dendrites of ramified microglia in *Cx<sub>3</sub>cr1<sup>+/gfp</sup> Ins2<sup>Akita</sup>* mice, demonstrating *Cx<sub>3</sub>cr1* deficiency combined with long-term diabetes affected all OPL microglia at this time point rather than a subpopulation of these cells. There were no reactive microglia in *Cx<sub>3</sub>cr1<sup>+/gfp</sup> Ins2<sup>Akita</sup>* mice at 10 weeks of age; however, 13% of OPL microglia were classified as reactive at 20 and 30 weeks. In comparison, 7% of OPL microglia were of reactive morphology in *Cx<sub>3</sub>cr1<sup>gfp/gfp</sup> Ins2<sup>Akita</sup>* mice at 10 weeks of age, 12.4% at 20 weeks, 27% at 30 weeks, and 20% at 46 weeks. These data indicated *Cx<sub>3</sub>cr1* deficiency may accelerate the morphologic changes to OPL microglia from a ramified to reactive form in the diabetic retina.

### *Cx<sub>3</sub>cr1* Deficiency Results in the Accumulation of Hyalocytes and Subretinal Macrophages in Diabetic Mice

Besides microglia in the parenchyma of the retina, the neural retina has two other closely related resident macrophage populations, hyalocytes on the vitread aspect (between the cortical vitreous and the inner aspect of the inner limiting membrane) and subretinal macrophages on the scleral aspect (among the photoreceptors and in the potential "space" between the photoreceptor outer segments and the apical retinal pigment epithelial surface). Previous studies in our laboratory have shown that hyalocyte number increases with age as well as in background retinopathy (*Ins2<sup>Akita</sup>* mice) and VEGF-driven retinal pathology (*Kimba* mice).<sup>29</sup> Additionally, we and others have demonstrated the age-related increase in subretinal macrophage number, which is accelerated in *Cx<sub>3</sub>cr1*-deficient mice.<sup>32,35</sup> Our study gave us the opportunity to extend these observations using our newly developed "Green Akita" mice. Thus, cell densities of Iba-1<sup>+</sup> hyalocytes

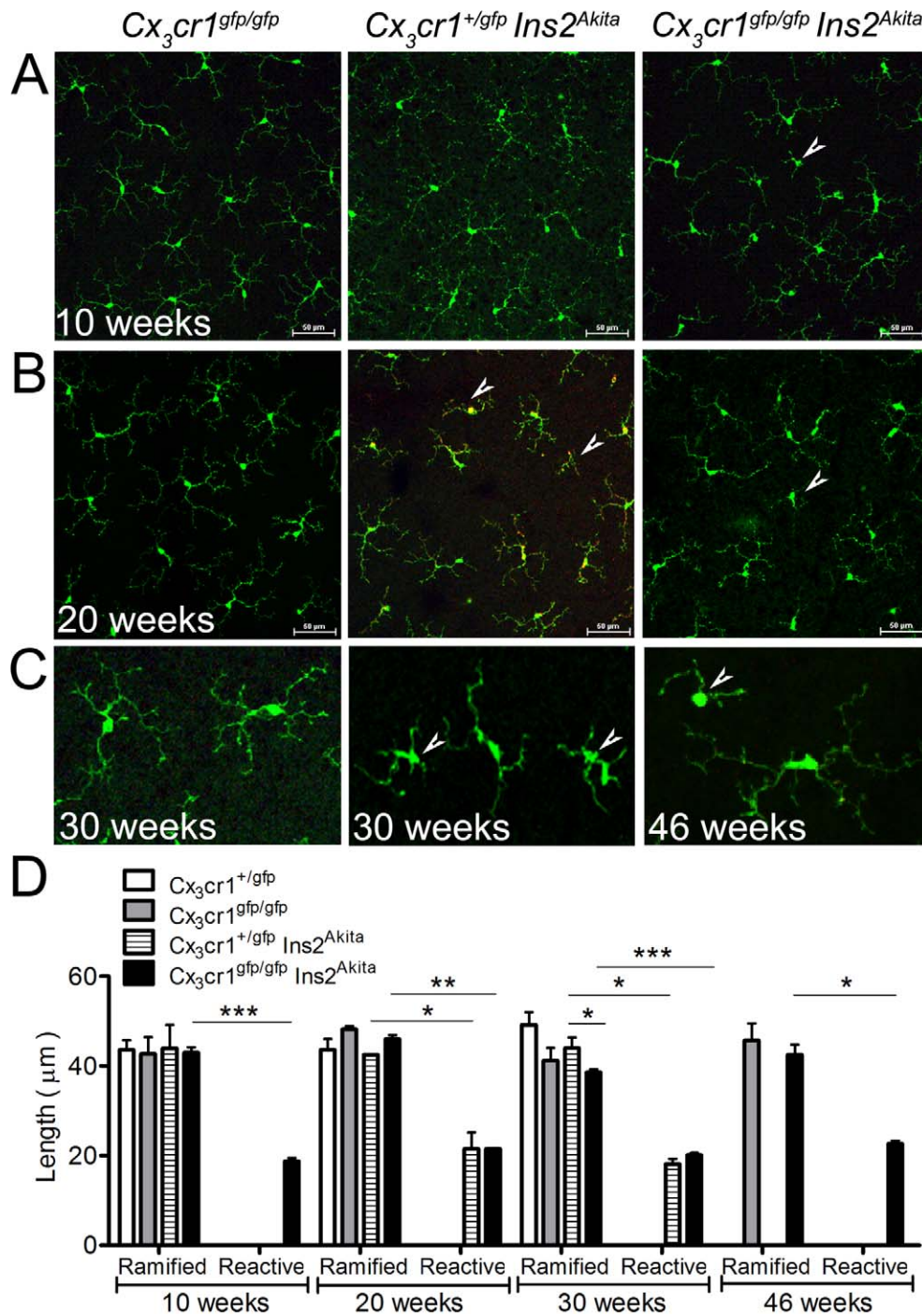


**FIGURE 5.** Changes to microglial morphology in *Ins2<sup>Akita</sup>* mice. Confocal microscopic images of retinal microglia in the OPL at 10 (A), 20 (B), 30 (C), and 46 (D) weeks of age. OPL microglia in diabetic mice had two distinct morphologies: ramified and reactive (A–C, arrowheads). Note the absence of reactive microglia in *Cx3cr1<sup>gfp/gfp</sup> Ins2<sup>Akita</sup>* at 10 weeks. The distance of primary dendrites from cell body (dendrite length) was calculated in OPL reactive and ramified microglia (D). Dendrite length of reactive microglia in diabetic mice was significantly less when compared to those of ramified microglia in all ages (D). At 30 weeks, dendrite length of ramified microglia was significantly less in *Cx3cr1<sup>gfp/gfp</sup> Ins2<sup>Akita</sup>* mice when compared to dendrite length of ramified microglia in *Cx3cr1<sup>+/gfp</sup> Ins2<sup>Akita</sup>* mice. Reactive microglia were not observed in nondiabetic mice. \**P* < 0.05, \*\**P* < 0.005, \*\*\**P* < 0.0005.

and subretinal macrophages were calculated on retinal whole mounts and compared between nondiabetic and diabetic groups. Diabetic status (*P* < 0.05) and *Cx3cr1* deficiency (*P* < 0.05) influenced the density of hyalocytes (Figs. 6A, 6C). Similarly, diabetic status (*P* < 0.05) and *Cx3cr1* deficiency (*P* < 0.05) led to a greater accumulation of Iba-1<sup>+</sup> cells in the subretinal space (Figs. 6B, 6C).

As the accumulation of these two populations of resident macrophage populations may reflect activation status and potentially migration of retinal microglia to supplement these populations, we next sought to determine whether immunophenotypic expression of putative activation markers on hyalocytes and subretinal macrophages was altered. In the naïve retina, hyalocytes express typical macrophage markers,

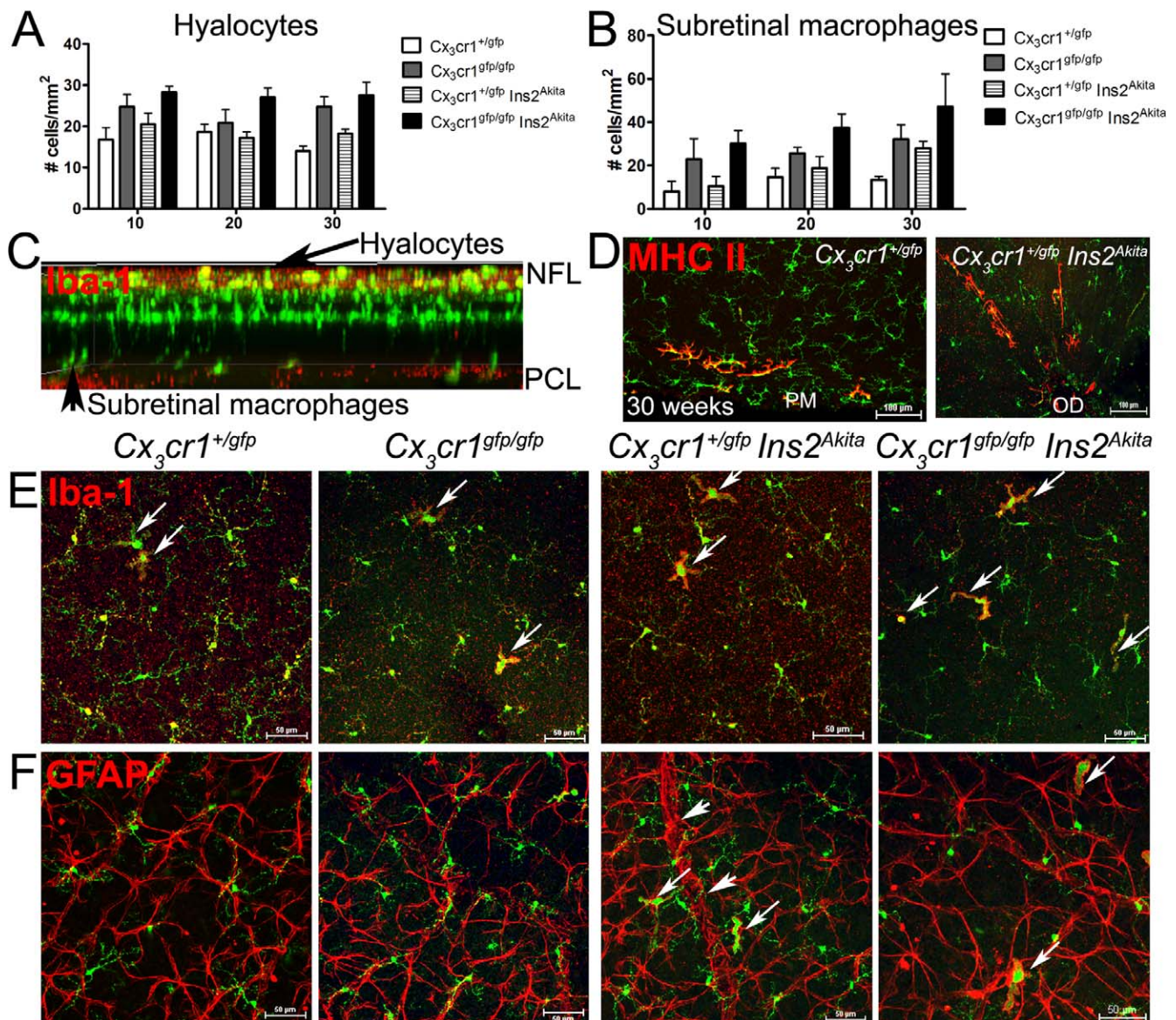


**FIGURE 6.** Changes in retinal macrophage cell density with age and *Cx3cr1* deficiency in *Ins2<sup>Akita</sup>* mice. Quantitative analysis of hyalocyte (A) and subretinal macrophage density (B) in 10-, 20-, and 30-week-old nondiabetic and diabetic mice. Diabetic status and *Cx3cr1* deficiency influenced the density of hyalocytes and subretinal macrophages ( $n = 4-6$  per genotype for each age group). (C) Confocal microscopic image representative of a whole retinal scan from NFL to PCL viewed in side profile, illustrating location of hyalocytes (arrow) and subretinal macrophages (arrowhead). Strong MHC Class II expression on perivascular macrophages at the peripheral margin ([D]; PM, left image) and optic disc ([D]; OD, right image). Confocal microscopic images representative of Iba-1 expression on hyalocytes ([E], arrows) and GFAP expression in the retina (F). GFAP was associated closely with hyalocytes ([F]; arrows) and blood vessels ([F], arrowheads) in diabetic mice. Green: GFP<sup>+</sup> microglia. Red: Iba-1<sup>+</sup>, MHC Class II<sup>+</sup> or GFAP<sup>+</sup> cells.

including Iba-1, F4/80, CD169 and CD11b, and upregulate MHC Class II expression during normal aging, in VEGF-driven proliferative retinopathy, or in response to systemic LPS exposure.<sup>29</sup> In our study, we did not detect MHC Class II expression on hyalocytes (Fig. 6D) or subretinal macrophages (not shown) in 10- to 30-week-old nondiabetic or diabetic mice. However, we noted more frequent expression of MHC Class II along perivascular microglia (sometimes referred to as perivascular macrophages) at the peripheral margin and optic disc region with increased age (Fig. 6D), independent of *Cx3cr1* deficiency or diabetic status. Strong expression of Iba-1 was observed on hyalocytes (Fig. 6E) and subretinal macrophages (not shown) in the retina across all age groups and genotypes, while isolectin-B4, a vascular marker also upregu-

lated by activated macrophages, was not expressed on either of these macrophage populations (not shown). GFAP expression on astrocytes was unchanged in diabetic mice, although GFAP was associated closely with the retinal vasculature and hyalocytes in diabetic mice (Fig. 6F).

#### Retinal Thickness Does Not Change in Diabetic *Ins2<sup>Akita</sup>* Mice Regardless of Age or *Cx3cr1* Deficiency

There has been some evidence that retinal thickness decreases in background retinopathy.<sup>9</sup> Peripheral and central retinal thicknesses were measured in sections of GMA-embedded eyes

from 10 to 46 weeks of age. No signs of retinal histopathology were observed in *Ins2<sup>Akita</sup>* mice at all time points examined (not shown). Statistical analysis revealed no significant differences in central or peripheral retinal thickness measurements with *Cx3cr1* deficiency or diabetic status across the age groups (see Supplementary Material and Supplementary Fig. S3, <http://www.iovs.org/lookup/suppl/doi:10.1167/iovs.12-10876/-/DCSupplemental>).

## DISCUSSION

Although considered traditionally a microvascular disease, it is becoming increasingly evident that DR has an inflammatory component, which is attributed partly to microglial reactivity. Changes in visual function also have been described in humans with background DR and in animal models of diabetes.<sup>38,39</sup> This correlates with the reported neuronal loss, as demonstrated by retinal thinning and increased rates of apoptosis in rodent models.<sup>9,40-42</sup> Interestingly, retinal neurodegeneration and microglial activation occur before the development of any vascular abnormalities or neuronal cell death.<sup>7,9</sup>

Our *in vivo* fundus examinations, as well as our *ex vivo* analysis of retinal whole mounts and resin histology, did not reveal signs of vascular leakage, leukostasis, inflammation, nor did we detect significant changes to retinal vascular morphology or retinal thickness in *Ins2<sup>Akita</sup>* mice. The measurement of retinal thicknesses using resin histology is considered preferable to conventional paraffin histology or cryosections, as resin embedding leads to only minor shrinkage of the tissue and produces high quality sections. One possible explanation for the discrepancies between our findings and previously reported neuronal loss, disruption of retinal morphology, and vascular changes in studies using *Ins2<sup>Akita</sup>* mice could be possible differences in bacterial flora in animal housing facilities. The microbial environment or exposure to microbial stimuli, as well as interactions between intestinal microbes and the innate immune system, have been shown to influence the development of spontaneous type I diabetes in nonobese diabetic (NOD) mice.<sup>43-46</sup> Another possible explanation for conflicting reports from studies using different colonies of *Ins2<sup>Akita</sup>* mice could be the presence of the *rd8* mutation in the *Crb1* gene,<sup>28</sup> a recently identified mutation that results in a retinal degeneration phenotype that has compromised numerous ocular research studies. According to Jax labs (available in the public domain at <http://jaxmice.jax.org/strain/003548.html>), the original *Ins2<sup>Akita</sup>* mouse colonies were produced from the C57BL/6JN strain and were not backcrossed completely onto the C57BL/6J strain until 2003. In light of this, we performed genotyping and sequencing of our *Cx3cr1<sup>+gfp</sup>*, *Cx3cr1<sup>gfp/gfp</sup>*, *Ins2<sup>Akita</sup> Cx3cr1<sup>+gfp</sup>*, and *Ins2<sup>Akita</sup> Cx3cr1<sup>gfp/gfp</sup>* mouse colonies, and found no *rd8* mutation, confirming their C57BL/6J background (not shown). The *rd8* status of *Ins2<sup>Akita</sup>* mice used in previous studies was not reported at the time.<sup>9</sup>

Our study tested the hypothesis that deficiency in *Cx3cr1*, known to be involved in the recruitment of myeloid-derived cells in homeostasis and inflammation,<sup>25,26,47,48</sup> would manifest as microglial changes or the development of characteristic diabetic retinopathy changes in the *Ins2<sup>Akita</sup>* mouse. The novel crossing of *Ins2<sup>Akita</sup>* mice with *Cx3cr1*-eGFP transgenic mice,<sup>22</sup> which were bred to test this hypothesis, had the advantage of greatly facilitating the long-term *in vivo* clinical examination of retinal microglia. It also negated the need for immunostaining to examine microglial networks in retinal whole mount studies, which can be highly variable due to differences in tissue processing techniques and staining protocols between

laboratory groups, as well as issues with antibody penetration, particularly in thicker tissue whole mounts, such as the retina.

The role of the chemokine receptor, *Cx3cr1*, in controlling microglial neurotoxicity has been well established in brain studies, with *Cx3cr1* deficiency having either neuroprotective or detrimental effects. In mouse models of LPS-induced inflammation, amyotrophic lateral sclerosis, and Parkinson's disease, the loss of signaling between *Cx3cr1<sup>+</sup>* microglia and *Cx3cl1* expressing neurons resulted in increased neuronal loss.<sup>23</sup> In contrast, *Cx3cr1* deficiency reduced  $\beta$ -amyloid deposition and prevented neuronal loss in models of Alzheimer's disease.<sup>49,50</sup> The effect of *Cx3cr1* deficiency on retinal microglia during ocular disease or inflammation is less clear. For example, while some report increased disease severity of experimental autoimmune uveitis in the absence of *Cx3cr1*,<sup>51</sup> we have shown *Cx3cr1* does not influence greatly disease pathogenesis.<sup>31</sup> Additionally, *Cx3cr1* deficiency does not affect the normal development of neurons, microglia, or the vasculature, and does not appear to alter the repair response to ischemic retinopathy.<sup>52</sup>

In our study, we noted a marked disruption in the regular laminar arrangement of retinal microglia in *Ins2<sup>Akita</sup>* mice. In diabetic mice, microglia in the IPL and OPL had abnormal cell processes extending through the nuclear layers, which became more marked with age. This disruption of microglial architecture may indicate increased microglial interactions or migrations between the retinal layers in diabetic mice, and may account for the increased densities of hyalocytes and subretinal macrophages at the vitread and scleral retinal interfaces. As proposed in our original hypothesis, these morphologic changes in microglia were more pronounced in diabetic retinopathy that lacked the chemokine receptor *Cx3cr1*. The significance of these retinal microglial changes, and why only a subpopulation of microglia are affected in conditions of hyperglycemia are yet to be elucidated, but it does raise the intriguing possibility that polymorphisms in genes involved in myeloid cell function may explain variations in susceptibility to diabetic retinopathy. One limitation of our study was the lack of data on pro-inflammatory markers in the retina in our "Green Akita" mice during aging and in the absence of *Cx3cr1* in this experimental cohort. However, in parallel studies we have failed to find any difference in mRNA levels of IL-1 $\beta$ , TNF- $\alpha$ , ICAM-1, and CD18 between *Ins2<sup>Akita</sup>* and WT mice at 7 and 18 weeks of age (unpublished data). Accordingly, future animal studies aimed at determining the functional significance of a reactive microglial phenotype will assess whether the cytokine profile of retinal microglia following stimulation with various toll-like receptor ligands is altered in the diabetic versus the nondiabetic retina.

An incidental finding in our study was the apparent delay in the full onset of a diabetic phenotype in *Cx3cr1*-deficient *Ins2<sup>Akita</sup>* mice at 10 weeks of age. Interestingly, we did not observe signs of polydipsia, polyurea, or weight loss in "Green Akita" mice, despite their confirmed diabetic status. We propose that the altered expression of typical diabetic features could be due to *Cx3cr1<sup>+gfp</sup>* mice expressing an intermediate phenotype between wild-type (WT) and *Cx3cr1<sup>gfp/gfp</sup>* mice, which may be due to increased tissue and circulating levels of *Cx3cl1*, the specific ligand for *Cx3cr1*. Cardona et al. demonstrated increased circulating *Cx3cl1*, as well as increased soluble *Cx3cl1* in CNS tissues of *Cx3cr1<sup>gfp/gfp</sup>* transgenic mice when compared to WT mice, and attributed this to a failure to clear excess ligand.<sup>53</sup> Interestingly, increased expression of *Cx3cl1* and *Cx3cr1* mRNA has been demonstrated in the kidney of streptozotocin-induced diabetic rats,<sup>54</sup> and a potential link between *Cx3cl1* and obesity-related type 2 diabetes in humans has been proposed.<sup>55</sup> We postulate that the normal expression of *Cx3cl1* in the eye may be altered during diabetes, and higher



constitutive levels of Cx<sub>3</sub>cl1 may, in fact, protect the eye from vascular damage. Thus, it is plausible that elevated Cx<sub>3</sub>cl1 levels in Cx<sub>3</sub>cr1<sup>+/sgfp</sup> and Cx<sub>3</sub>cr1<sup>sgfp/sgfp</sup> mice as suggested by Cardona et al.<sup>53</sup> may explain partly the altered diabetic phenotype of “Green Akita” mice and absence of vascular changes associated with long-term diabetes in this study.

### Acknowledgments

We thank the staff at the Monash Micro Imaging (MMI) facility, Monash University, for their technical assistance with confocal microscopy and Imaris software.

### References

- Klein BE. Overview of epidemiologic studies of diabetic retinopathy. *Ophthalmic Epidemiol.* 2007;14:179-183.
- Aiello LP, Gardner TW, King GL, et al. Diabetic retinopathy. *Diabetes Care.* 1998;21:143-156.
- Kempner JH, O'Colmain BJ, Leske MC, et al. The prevalence of diabetic retinopathy among adults in the United States. *Arch Ophthalmol.* 2004;122:552-563.
- Cheung N, Mitchell P, Wong TY. Diabetic retinopathy. *Lancet.* 2010;376:124-136.
- Huang H, Gandhi JK, Zhong X, et al. TNFalpha is required for late BRB breakdown in diabetic retinopathy, and its inhibition prevents leukostasis and protects vessels and neurons from apoptosis. *Invest Ophthalmol Vis Sci.* 2011;52:1336-1344.
- Villaruel M, Ciudin A, Hernandez C, Simo R. Neurodegeneration: an early event of diabetic retinopathy. *World J Diabetes.* 2010;1:57-64.
- Gaucher D, Chiappore JA, Paques M, et al. Microglial changes occur without neural cell death in diabetic retinopathy. *Vision Res.* 2007;47:612-623.
- Tang J, Kern TS. Inflammation in diabetic retinopathy. *Prog Retin Eye Res.* 2011;30:343-358.
- Barber AJ, Antonetti DA, Kern TS, et al. The Ins2Akita mouse as a model of early retinal complications in diabetes. *Invest Ophthalmol Vis Sci.* 2005;46:2210-2218.
- Nimmerjahn A, Kirchhoff F, Helmchen F. Resting microglial cells are highly dynamic surveillants of brain parenchyma in vivo. *Science.* 2005;308:1314-1318.
- Magnus T, Chan A, Grauer O, Toyka KV, Gold R. Microglial phagocytosis of apoptotic inflammatory T cells leads to down-regulation of microglial immune activation. *J Immunol.* 2001;167:5004-5010.
- Ransohoff RM, Perry VH. Microglial physiology: unique stimuli, specialized responses. *Annu Rev Immunol.* 2009;27:119-145.
- Jurgens HA, Johnson RW. Dysregulated neuronal-microglial cross-talk during aging, stress and inflammation. *Exp Neurol.* 2012;233:40-48.
- Karlstetter M, Ebert S, Langmann T. Microglia in the healthy and degenerating retina: insights from novel mouse models. *Immunobiology.* 2010;215:685-691.
- Weitz TM, Town T. Microglia in Alzheimer's disease: it's all about context. *Int J Alzheimer's Dis.* 2012;2012:314185.
- Gao Z, Tsirka SE. Animal models of MS reveal multiple roles of microglia in disease pathogenesis. *Neurol Res Int.* 2011;2011:383087.
- Gonzalez-Scarano F, Baltuch G. Microglia as mediators of inflammatory and degenerative diseases. *Annu Rev Neurosci.* 1999;22:219-240.
- Zeng HY, Green WR, Tso MO. Microglial activation in human diabetic retinopathy. *Arch Ophthalmol.* 2008;126:227-232.
- Cukras CA, Petrou P, Chew EY, Meyerle CB, Wong WT. Oral minocycline for the treatment of diabetic macular edema (DME): results of a phase i/ii clinic study. *Invest Ophthalmol Vis Sci.* 2012;53:3865-3874.
- Kreutzberg GW. Microglia: a sensor for pathologic events in the CNS. *Trends Neurosci.* 1996;19:312-318.
- Santos AM, Martin-Oliva D, Ferrer-Martin RM, et al. Microglial response to light-induced photoreceptor degeneration in the mouse retina. *J Comp Neurol.* 2010;518:477-492.
- Jung S, Aliberti J, Graemmel P, et al. Analysis of fractalkine receptor CX(3)CR1 function by targeted deletion and green fluorescent protein reporter gene insertion. *Mol Cell Biol.* 2000;20:4106-4114.
- Cardona AE, Piro EP, Sasse ME, et al. Control of microglial neurotoxicity by the fractalkine receptor. *Nat Neurosci.* 2006;9:917-924.
- Kezic J, Xu H, Chinnery HR, Murphy CC, McMenamin PG. Retinal microglia and uveal tract dendritic cells and macrophages are not CX3CR1 dependent in their recruitment and distribution in the young mouse eye. *Invest Ophthalmol Vis Sci.* 2008;49:1599-1608.
- Chinnery HR, Ruitenberg MJ, Plant GW, Pearlman E, Jung S, McMenamin PG. The chemokine receptor CX3CR1 mediates homing of MHC class II-positive cells to the normal mouse corneal epithelium. *Invest Ophthalmol Vis Sci.* 2007;48:1568-1574.
- Huang D, Shi FD, Jung S, et al. The neuronal chemokine CX3CL1/fractalkine selectively recruits NK cells that modify experimental autoimmune encephalomyelitis within the central nervous system. *FASEB J.* 2006;20:896-905.
- Rakoczy EP, Ali Rahman IS, Binz N, et al. Characterization of a mouse model of hyperglycemia and retinal neovascularization. *Am J Pathol.* 2010;177:2659-2670.
- Mattapallil MJ, Wawrousek EF, Chan CC, et al. The Rd8 mutation of the Crb1 gene is present in vendor lines of C57BL/6N mice and embryonic stem cells, and confounds ocular induced mutant phenotypes. *Invest Ophthalmol Vis Sci.* 2012;53:2921-2927.
- Vagaja NN, Chinnery HR, Binz N, Kezic JM, Rakoczy EP, McMenamin PG. Changes in murine hyalocytes are valuable early indicators of ocular disease. *Invest Ophthalmol Vis Sci.* 2012;53:1445-1451.
- McMenamin PG. Optimal methods for preparation and immunostaining of iris, ciliary body, and choroidal whole-mounts. *Invest Ophthalmol Vis Sci.* 2000;41:3043-3048.
- Kezic J, McMenamin PG. The monocyte chemokine receptor CX3CR1 does not play a significant role in the pathogenesis of experimental autoimmune uveoretinitis. *Invest Ophthalmol Vis Sci.* 2010;51:5121-5127.
- Chinnery HR, McLenachan S, Humphries T, et al. Accumulation of murine subretinal macrophages: effects of age, pigmentation and CX3CR1. *Neurobiol Aging.* 2011;33:1769-1776.
- Combadiere C, Feumi C, Raoul W, et al. CX3CR1-dependent subretinal microglia cell accumulation is associated with cardinal features of age-related macular degeneration. *J Clin Invest.* 2007;117:2920-2928.
- Luhmann UF, Robbie S, Munro PM, et al. The drusenlike phenotype in aging Ccl2-knockout mice is caused by an accelerated accumulation of swollen autofluorescent subretinal macrophages. *Invest Ophthalmol Vis Sci.* 2009;50:5934-5943.
- Xu H, Chen M, Manivannan A, Lois N, Forrester JV. Age-dependent accumulation of lipofuscin in perivascular and subretinal microglia in experimental mice. *Aging Cell.* 2008;7:58-68.
- Lee JE, Liang KJ, Fariss RN, Wong WT. Ex vivo dynamic imaging of retinal microglia using time-lapse confocal microscopy. *Invest Ophthalmol Vis Sci.* 2008;49:4169-4176.

37. Vessey KA, Greferath U, Jobling AI, et al. Ccl2/Cx3cr1 knockout mice have inner retinal dysfunction but are not an accelerated model of age related macular degeneration. *Invest Ophthalmol Vis Sci*. 2012;53:7833-7846.
38. Akimov NP, Renteria RC. Spatial frequency threshold and contrast sensitivity of an optomotor behavior are impaired in the *Ins2Akita* mouse model of diabetes. *Behav Brain Res*. 2012;226:601-605.
39. Shirao Y, Kawasaki K. Electric responses from diabetic retina. *Prog Retin Eye Res*. 1998;17:59-76.
40. Barber AJ, Gardner TW, Abcouwer SF. The significance of vascular and neural apoptosis to the pathology of diabetic retinopathy. *Invest Ophthalmol Vis Sci*. 2011;52:1156-1163.
41. Smith SB, Duplantier J, Dun Y, et al. In vivo protection against retinal neurodegeneration by sigma receptor 1 ligand (+)-pentazocine. *Invest Ophthalmol Vis Sci*. 2008;49:4154-4161.
42. Martin PM, Roon P, Van Ells TK, Ganapathy V, Smith SB. Death of retinal neurons in streptozotocin-induced diabetic mice. *Invest Ophthalmol Vis Sci*. 2004;45:3330-3336.
43. Wen L, Ley RE, Volchkov PY, et al. Innate immunity and intestinal microbiota in the development of type 1 diabetes. *Nature*. 2008;455:1109-1113.
44. Sadelain MW, Qin HY, Lauzon J, Singh B. Prevention of type 1 diabetes in NOD mice by adjuvant immunotherapy. *Diabetes*. 1990;39:583-589.
45. Sadelain MW, Qin HY, Sumoski W, Parfrey N, Singh B, Rabinovitch A. Prevention of diabetes in the BB rat by early immunotherapy using Freund's adjuvant. *J Autoimmun*. 1990;3:671-680.
46. Pozzilli P, Signore A, Williams AJ, Beales PE. NOD mouse colonies around the world - recent facts and figures. *Immunol Today*. 1993;14:193-196.
47. Niess JH, Brand S, Gu X, et al. CX3CR1-mediated dendritic cell access to the intestinal lumen and bacterial clearance. *Science*. 2005;307:254-258.
48. Ruitenbergh MJ, Vukovic J, Blomster L, et al. CX3CL1/fractalkine regulates branching and migration of monocyte-derived cells in the mouse olfactory epithelium. *J Neuroimmunol*. 2008;205:80-85.
49. Lee S, Varvel NH, Konecny ME, et al. CX3CR1 deficiency alters microglial activation and reduces beta-amyloid deposition in two Alzheimer's disease mouse models. *Am J Pathol*. 2010;177:2549-2562.
50. Fuhrmann M, Bittner T, Jung CK, et al. Microglial Cx3cr1 knockout prevents neuron loss in a mouse model of Alzheimer's disease. *Nat Neurosci*. 2010;13:411-413.
51. Dagkalis A, Wallace C, Hing B, Liversidge J, Crane IJ. CX3CR1-deficiency is associated with increased severity of disease in experimental autoimmune uveitis. *Immunology*. 2009;128:25-33.
52. Zhao L, Ma W, Fariss RN, Wong WT. Retinal vascular repair and neovascularization are not dependent on CX3CR1 signaling in a model of ischemic retinopathy. *Exp Eye Res*. 2009;88:1004-1013.
53. Cardona AE, Sasse ME, Liu L, et al. Scavenging roles of chemokine receptors: chemokine receptor deficiency is associated with increased levels of ligand in circulation and tissues. *Blood*. 2008;112:256-263.
54. Kikuchi Y, Ike R, Hemmi N, et al. Fractalkine and its receptor, CX3CR1, upregulation in streptozotocin-induced diabetic kidneys. *Nephron*. 2004;97:e17-e25.
55. Shah R, Hinkle CC, Ferguson JF, et al. Fractalkine is a novel human adipokine associated with type 2 diabetes. *Diabetes*. 2011;60:1512-1518.